The effect of water uptake on the mechanical properties of low-k organosilicate glass

X. Guo, J. E. Jakes, M. T. Nichols, S. Banna, Y. Nishi et al.

Citation: J. Appl. Phys. **114**, 084103 (2013); doi: 10.1063/1.4817917
View online: http://dx.doi.org/10.1063/1.4817917
View Table of Contents: http://jap.aip.org/resource/1/JAPIAU/v114/i8
Published by the AIP Publishing LLC.

The effect of water uptake on the mechanical properties of low-k organosilicate glass

X. Guo,[1] J. E. Jakes,[2] M. T. Nichols,[1] S. Banna,[3] Y. Nishi,[4] and J. L. Shohet[1]
[1]*Plasma Processing & Technology Laboratory and Department of Electrical and Computer Engineering, University of Wisconsin-Madison, Madison, Wisconsin 53706, USA*
[2]*Forest Biopolymer Science and Engineering, USDA Forest Service Forest Products Laboratory, Madison, Wisconsin 53726, USA*
[3]*Applied Materials, Sunnyvale, California 94085, USA*
[4]*Stanford University, Stanford, California 94305, USA*

(Received 25 June 2013; accepted 26 July 2013; published online 23 August 2013)

Water uptake in porous low-k dielectrics has become a significant challenge for both back-end-of-line integration and circuit reliability. The influence of absorbed water on the mechanical properties of plasma-enhanced chemical-vapor-deposited organosilicate glasses (SiCOH) was investigated with nanoindentation. The roles of physisorbed (α-bonded) and chemisorbed (β-bonded) water were examined separately through annealing at different temperatures. Nanoindentation measurements were performed on dehydrated organosilicate glass during exposure to varying humidity conditions. The elastic modulus and hardness for as-deposited SiCOH are intimately linked to the nature and concentration of the absorbed water in the dielectric. Under mild-annealing conditions, the water-related film mechanical property changes were shown to be reversible. The mechanical properties of UV-cured SiCOH were also shown to depend on absorbed water, but to a lesser extent because UV curing depopulates the hydrophilic chemical groups in SiCOH. High-load indentation tests showed that in-diffusion of water in the film/substrate interface can degrade the hardness of SiCOH/Si film stacks significantly, while not significantly changing the elastic modulus.
 [http://dx.doi.org/10.1063/1.4817917]

I. INTRODUCTION

Interconnect resistive-capacitive (RC) delay is a major challenge for the further downscaling of integrated circuits. To reduce the capacitance, materials with lower dielectric constants are being used in back-end-of-line (BEOL) integration. Recently, low-k porous organosilicate glasses (OSG or SiCOH), i.e., porous SiO_2 with hydrophobic methyl groups ($-CH_3$) lining the pores, have attracted much attention and are widely accepted due to their enormous potential as an alternative to conventional SiO_2 for inter-metal dielectrics.[1–3] However, these originally hydrophobic porous-structured low-k dielectrics have been found to become hydrophilic after plasma processing (e.g., photoresist stripping and cleaning).[4] For example, CF_x polymers that are deposited during the etching of SiCOH in fluorocarbon plasma can introduce hydrophilic properties to SiCOH because they are not as hydrophobic as $-CH_3$ groups. Additionally, oxygen plasma, usually used to remove organic photoresist polymers, can also remove the original hydrophobic groups ($-CH_3$) and create some free radical sites ($-SiO_2\bullet$), resulting in the formation of hydrophilic $-SiO_2$-OH groups. These hydrophilic groups enable significant amounts of water to be absorbed from humid air following diffusion into the SiCOH bulk through interconnected pores.[5]

During the interconnect fabrication process, wafers are repeatedly exposed to aqueous solutions[6] and significant amounts of water can be adsorbed and then diffuse into low-k dielectric films, by attaching to different chemical groups in the skeleton. This will degrade the dielectric properties and worsen reliability.[7] Thus, water uptake in porous low-k dielectrics is a significant challenge for both BEOL integration and circuit reliability. In order to optimize the integration processes that can lower the mobility of water molecules and minimize the effect of moisture, it is critical to understand the fundamental interactions between moisture and low-k dielectrics. Much work has been done to investigate the moisture absorption and transport mechanisms in low-k dielectrics and the effects of absorbed water on the material's electrical properties and reliability.[8,9] Previous work[9] attempting to evaluate the effect of humidity on the mechanical response of these low-k dielectrics has shown that both the film hardness and elastic modulus can significantly vary with ambient humidity, and these effects cannot be explained easily by considering pore filling and/or stiffening associated with capillary stress. The actual mechanism and influence of various absorbed water components on the mechanical properties of SiCOH are still obscure. This knowledge has the potential to result in some important implications for fabrication of interconnect structures, such as post-processing of the film/substrate interface in dielectric film stacks.

Another concern is the change in mechanical properties induced by moisture uptake in ultraviolet (UV) cured SiCOH. As a promising treatment for strengthening porous low-k materials, UV curing can improve the chemical stability and the mechanical properties of plasma-enhanced chemical-vapor-deposited (PECVD) SiCOH films by rearrangement of their bond structures. For example, the UV-curing process decreases the number of terminal non-bridging bonds and

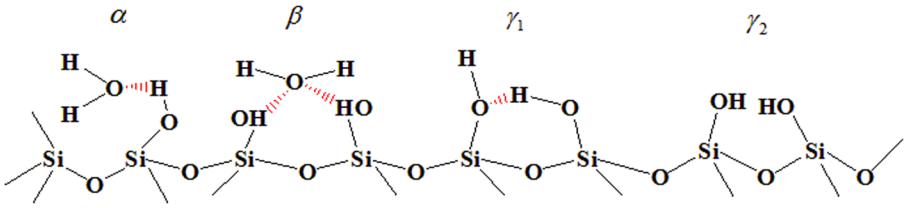

FIG. 1. Schematic drawing of the various OH species existed in Si-based organosilicate glass and their bond types to siloxane groups.

increases the number of cross-linking bonds.[10] This rearrangement strengthens the bulk Si–O–Si backbone and leads to significant increases in elastic modulus and interfacial fracture energy.[11] In addition, structural rearrangement was seen to occur at the film surface and a SiO_2-like layer can form there.[12] Since the water solubility and diffusivity in the SiO_2-like layer are different from the bulk, the moisture intrusion and retention behavior in UV-cured low-k films is believed to be different.[13] For these reasons, it is useful to make a further investigation into the influence of water uptake on the mechanical properties of UV-cured SiCOH.

In this work, the influence of moisture uptake on the mechanical properties of both as-deposited and UV-cured organosilicate glass is investigated and the roles of separate absorbed water components were analyzed separately. For this purpose, PECVD SiCOH was pretreated with plasma for demethylation/hypomethylation and to increase the number of hydrophilic groups in the low-k films. After exposure to a humid ambient, separate annealing temperatures and procedures were chosen so as to dehydrate separate water components out of these hydrophilic samples. Fourier-transformed infrared spectroscopy (FTIR) was used to monitor the effectiveness of the dehydration. Then, nanoindentation tests were performed on the annealed samples in a sealed chamber with low relative humidity (RH). To identify the influence of different water components, the same measurements were repeated after conditioning the film at higher RH's, in which case water again enters into the annealed samples and diffuses into the bulk. In addition, a high-load indentation test was also carried out on a variety of annealed samples, enabling the characterization of the effect of in-diffused water at the film/substrate interface.

II. EXPERIMENT

A. Materials preparation

The low-k dielectric materials used in this work were PECVD porous SiCOH films ($k \approx 2.55$, organosilane precursor), whose as-deposited thickness was 644 nm. UV curing was performed using a Novellus SOLA Ultraviolet Thermal Processing (UVTP) system. The film thickness after UV-curing was measured using an ellipsometer to be 500 nm. An electron cyclotron resonance (ECR) plasma system[14] operating with a 400 W, 2.45 GHz microwave power source and an 875 G magnetic field was utilized for plasma exposure. The feed gas was an argon-oxygen mixture ($Ar/O_2 = 50/50$), and the operating pressure was 10 mTorr. The exposure time was set to 100 s to ensure efficient demethylation and to avoid significant generation of other plasma-induced damage. Both as-deposited and UV-cured SiCOH were exposed under the same conditions.

For these dielectrics, which include free radical sites ($-SiO_2\bullet$), it has been reported that there exist four types of water-related chemical groups attached to the Si-based siloxane groups, as shown in Figure 1.[15] The α-bonded and β-bonded water components, often called physisorbed water and chemisorbed water, respectively, are water molecules that are hydrogen-bonded to the hydrophilic hydroxyl groups. Unlike α-bonded water molecules that are loosely bonded to each other and to surface hydroxyl groups, β-bonded water is tightly hydrogen-bonded to two neighboring hydroxyl groups. The existence of these water molecules will increase the dielectric constant of the material and thus detract from efforts to develop low-k dielectrics. Fortunately, these hydrogen-bonded water components can be desorbed at a specific annealing temperature, without changing or damaging the chemical structure and integrity of the SiCOH.[1,16]

The associated reactions for four separate water component desorption mechanisms are shown in Eqs. (1)–(4).[7] Table I lists the desorption activation energy E_a (enthalpy of activation) for the different water components. E_a enables a quantitative comparison with the enthalpy of water condensation, to determine the desorption temperature of water in different absorbed states.

$$\alpha: \equiv Si - OH \cdots H_2O \rightarrow \equiv Si - OH + H_2O, \quad (1)$$

$$\beta: \equiv Si - OH \cdots H_2O \cdots OH - Si \equiv \rightarrow 2 \equiv Si - OH + H_2O, \quad (2)$$

$$\gamma_1: \equiv Si - OH \cdots OH - Si \equiv \rightarrow \equiv Si - O - Si \equiv + H_2O, \quad (3)$$

$$\gamma_2: \equiv Si - OH + OH - Si \equiv \rightarrow \equiv Si - O - Si \equiv + H_2O. \quad (4)$$

In this work, two different annealing temperatures were selected to remove the hydrogen-bonded water from hydroxyl groups in SiCOH. The first one was 190 °C, which can remove the α-bonded water component, and at the same time leaving the β-bonded water component still connected to hydroxyl groups. The second annealing temperature was 400 °C, which removes both residual α- and β-bonded water

TABLE I. Arrhenius parameters for the different elementary water desorption mechanisms.

Water component	E_a (kJ/mol)	Assignment
α	23 ± 2	Physisorbed water
β	55 ± 17	Tightly hydrogen-bonded water[a]
γ_1	89 ± 1	Hydrogen-bonded silanol
γ_2	202 ± 18	Isolated silanol

[a]Tightly hydrogen-bonded water here is so-called chemisorbed water.
[b]The values come from Ref. 7.

components existing in SiCOH.[7] The annealing time was set to be 1 h, based on the moisture absorption and desorption dynamics model of Yao *et al.*[13]

A temperature-programmable oven was used as the annealing system. To guarantee the annealing process indeed removes the different absorbed water components effectively and at the same time did not change the chemical structure of the low-k SiCOH films, a specific annealing procedure was adopted and run in three stages: (1) initial water absorption; (2) N_2 purging and annealing, and (3) final cooling down and vacuum packing.

For stage 1, since water absorption by porous dielectrics occurs readily upon exposure to air, the samples were exposed to high moisture content air (about 80% RH) at room temperature for 60 h, which is longer than the predicted time from the model of Yao *et al.*, to make sure the hydrophilic SiCOH film was water-saturated. For stage 2, the oven chamber was purged with dry semiconductor-grade nitrogen gas with temperatures up to 120 °C for 10 min before starting annealing, to reduce the background moisture and impurity levels, which could contaminate the films. Then, the annealing process was started. The water-saturated samples were heated with infrared lamps and the temperature was ramped up from room temperature to either 190 °C or 400 °C at a constant rate of 0.2 °C/s, to minimize the possibility of film delamination from the substrate. The samples were kept in flowing dry nitrogen gas for 1 h after the temperature reached its designated level of 190 °C/400 °C. The dry N_2 flow rate was kept stable at 10^3 sccm, so that water driven out from the films was carried away to avoid reabsorption or contamination. After the heating process, for stage 3, the samples were kept in the chamber to cool down to room temperature with a dry N_2 flow rate of 10^2 sccm and vacuum packaged.

As a control, some samples were heated to only 100 °C. This procedure was designed to remove the water adhering to the sample surface and to minimize influences on the measurement results from capillary stresses.[17,18] During this annealing step, the absorbed α- and β-bonded water components should not be affected and the samples remained water saturated.

FTIR measurements were conducted on the annealed samples, allowing detailed insight into the changes in SiCOH. Figure 2 shows the measured FTIR of water-saturated SiCOH and annealed SiCOH for the two annealing temperatures. Table II summarizes the −OH relative absorbance peaks in PECVD SiCOH low-k films.[19] Information about the behavior of absorbed α- and β-bonded water components after annealing can be obtained by tracking and comparing these −OH related peaks. As is shown in Figure 2(a), water-saturated as-deposited SiCOH indicates the existence of abundant hydrophilic groups during processing. For films annealed at 190 °C, the spectrum shows a lower peak height of the −OH related features, together with a moderate shift toward higher wavenumbers of the stretching modes of isolated and terminal −OH bonds (3650–3800 cm^{-1}).

This can be explained as follows. The annealing process removes the H-bonded H_2O but not the terminal hydroxyl that is bonded to the Si-O chain. Since the stretching modes of isolated and terminal −OH have IR spectral peaks with higher wavenumbers, the detected −OH related peaks shift a little bit to the left, as shown in Figure 2(a). This trend is more significant for the film annealed at 400 °C, which has a lowest −OH related peak because of the loss of both α- and β-bonded water. These results are similar to the work of Kubasch *et al.*[20] and indicate that these absorbed water components can be removed effectively by annealing.

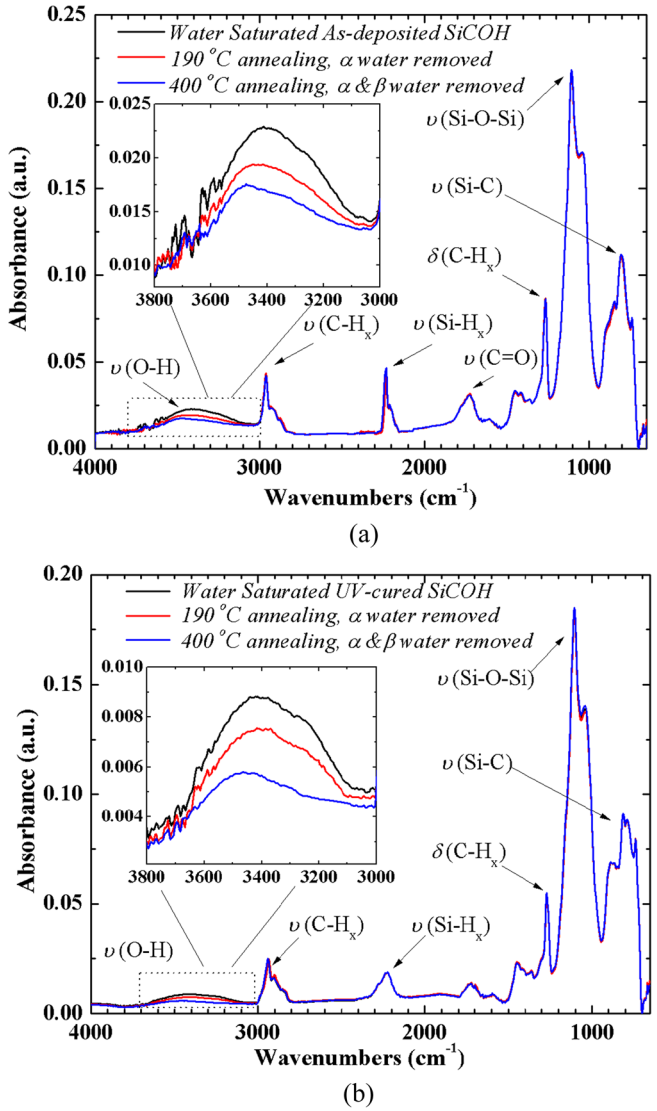

FIG. 2. (a) FTIR spectrum of the water-saturated, 190 °C annealed and 400 °C annealed as-deposited low-k SiCOH film; (b) FTIR spectrum of the water-saturated, 190 °C annealed and 400 °C annealed UV-cured low-k SiCOH film.

In addition, it was observed that for the 190 °C/400 °C annealed samples, the −OH related peaks increase and tend to approach the water-saturated level after exposing the

TABLE II. −OH related FTIR peak assignments in PECVD SiCOH low-k films.

Wavenumber (cm^{-1})	Comment
3300–3600	H-bonded H_2O (O-H stretching)
3650–3800	Stretching modes of isolated and terminal −OH
3690	Hydroxyl terminals
3750	Isolated surface silanols Si-OH (sharp peak)
3200–3650	H-bonded Si-OH in chain (Si-OH stretching)

samples to humid air. This indicates that in a highly humid environment, the dehydrated SiCOH can easily reabsorb water until saturation is reached.

The FTIR spectra of UV-cured SiCOH, as depicted in Figure 2(b), show almost the same results in the region between 3300 and 3800 cm^{-1}. It also can be noted that for both annealing temperatures, the other main FTIR peaks from the PECVD SiCOH, such as Si-O-Si (1068 cm^{-1}), C-H_x (1273 cm^{-1}, 2878 cm^{-1}, 2973 cm^{-1}), Si-H_x (2178 cm^{-1}, 2232 cm^{-1}), and Si-C (800 cm^{-1}), remain almost unchanged after annealing, indicating no measurable chemical structure change or damage occurs for these groups. The only variation in the SiCOH film induced by annealing is from the water components, and any property changes should be water related.

B. Nanoindentation measurements

Moisture-dependent elastic modulus (E_s), Meyer hardness (H), and fracture behavior of SiCOH films were investigated with a Hysitron (Minneapolis, MN, USA) TriboIndenter® equipped with a Berkovich probe. The RH inside the TriboIndenter enclosure was controlled with an InstruQuest (Coconut Creek, FL, USA) HumiSysTM HF RH generator. To minimize exposure to ambient humidity, the films were removed from their vacuum packaging and mounted with epoxy on 15 mm steel AFM pucks inside of a glove box with dry air flowing through it. Inside the glove box, the mounted films were sealed inside of containers that were carried to the TriboIndenter® enclosure preconditioned at 10% RH. Inside the TriboIndenter® enclosure the films were removed from the sealed containers and mounted on the TriboIndenter® stage as quickly as possible to minimize any changes in enclosure RH caused by the brief exposure to ambient RH. Nanoindentation was first performed at 10% RH, followed by 38% and 73% RH. The films were conditioned for a minimum of 24 h at each RH before testing. For each increased humidity level, measurements were repeated following the same procedure at different locations on the samples.

For each measurement, the indenter was operated in force-displacement mode and the tip oscillation frequency was 125 Hz. Machine compliance was assessed from a 0.01-1.2 mN series of load control indents in a fused silica standard using the SYS correlation.[21] Both calibration and SiCOH experiments utilized a load-control indent consisting of an initial 20 nm lift-off and reapproach in order to define the initial contact point accurately, followed by a 5 s loading, a 5 s hold at maximum load (P_{max}), a 2 s unloading to 40% of the P_{max}, a 60 s hold at 40% P_{max} to remove thermal drift effects, and a 1 s final unload. Figure 3(a) shows the load function and Figure 3(b) shows a typical series of indents performed in each SiCOH film at each RH. After correcting the fused silica load-depth traces for machine compliance, the series of indents were used to calculate the area function following the standard Oliver-Pharr method. All the nanoindentation experiments were carried out at room temperature.

C. SEM imaging

To monitor and evaluate the moisture-dependent fracture behavior of SiCOH, a Zeiss LEO 1530 field emission

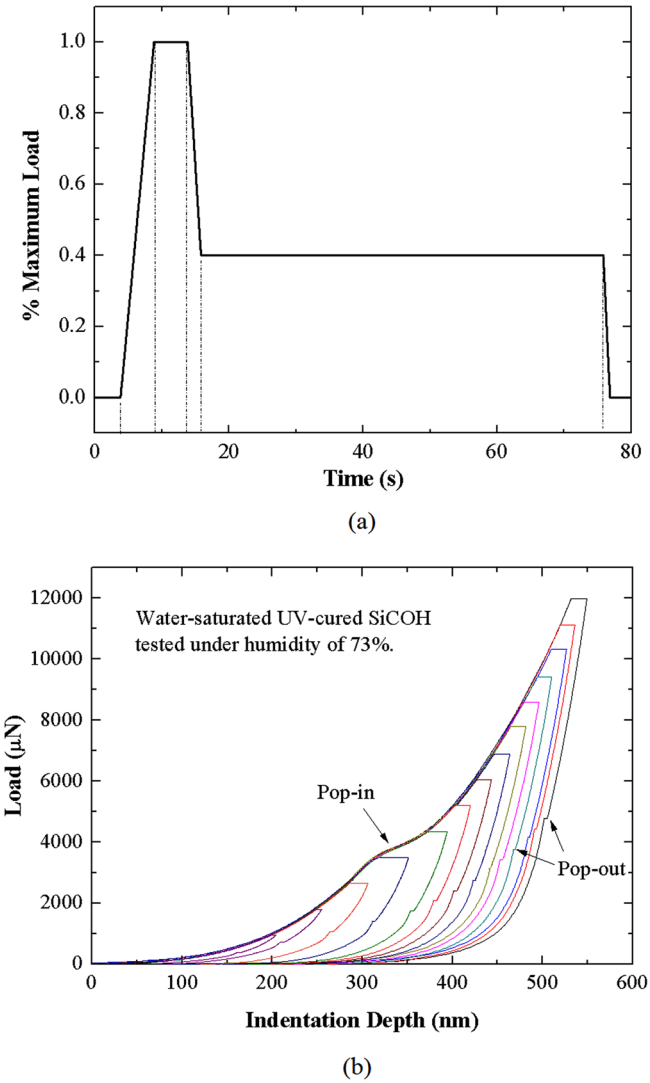

FIG. 3. (a) Load function used in this work, which consists of a 5 s loading, 5 s hold at maximum load, 2 s unload to 40% of the maximum load, 60 s hold at 40% maximum load, 1 s final unload, and a 4 s hold at zero load (The 60 s hold was used to correct the load-depth trace for thermal drift and the 4 s hold was used to assure the load was properly zeroed.); (b) load-depth traces for 20 indents performed on a 500 nm water-saturated UV-cured SiCOH film under humidity of 10%, arrow indicates the occurring of pop-in and pop-out event.

scanning electron microscope (SEM) was used to image all residual indents on the specimen surface. A very thin Au layer (~60 nm) was sputter-coated on each specimen for high-quality SEM imaging. Figure 4 is representative of the SEM images of residual indents with different P_{max}. During the indentation process, if the load is sufficiently high, a crack can be initiated from the indent corners and emanates along the direction of "contact radius," as depicted in Figs. 4(c) and 4(d). Cracks in the vicinity of the indents can be seen to lengthen and widen with increasing P_{max}, similar to the observations of other investigations for porous OSG low-k films.[22]

For each cracked indent, the length of fracture (c), defined as the distance from the indent corner to crack tip,[23] as shown in Fig. 4(c), was measured. Also, the critical load, the minimum load at which film fracture is

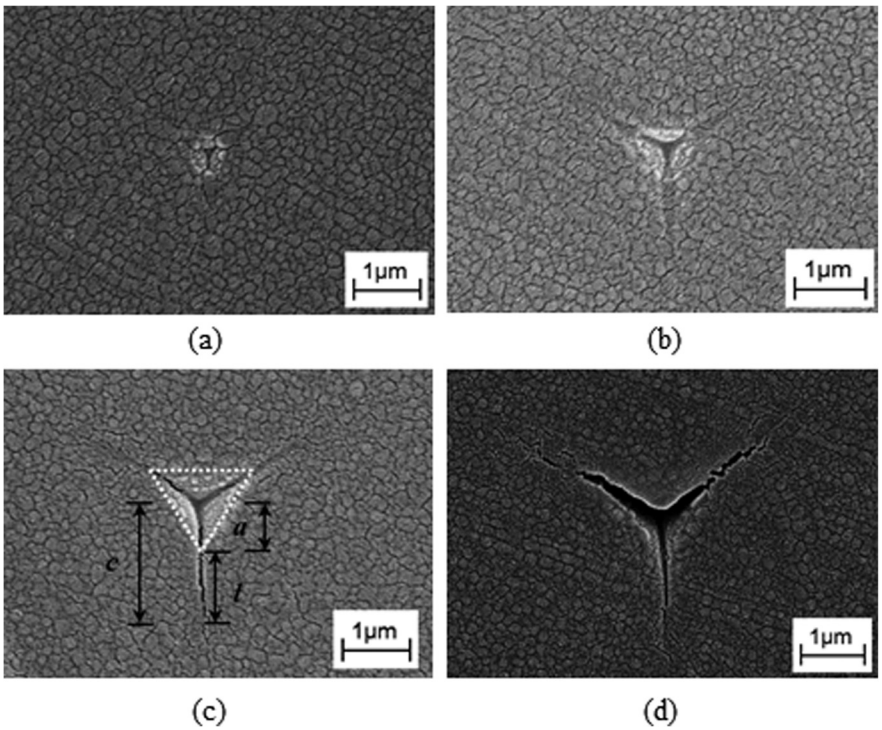

FIG. 4. SEM images of residual indents on the specimen surface with the maximum load of (a) 0.25 mN, (b) 0.50 mN, (c) 0.75 mN, and (d) 1.00 mN. Geometric parameters ***a***, ***l***, and ***c*** labeled in (c) are "contact radius," emanated crack length, and total crack length, respectively, where $\boldsymbol{c = a + l}$. All images are from the indents on water-saturated UV-cured SiCOH under humidity of 10%.

observed, was recorded and compared with each series of nanoindents.

III. RESULTS AND DISCUSSION

A. Nanoindentation analysis

From the experimentally obtained load-displacement curves during nanoindentation, the initial unloading stiffness ($S = dP/dh$) was assessed by fitting 40%–95% maximum load (P_{max}) of the unloading P-h segment to a power law $P = A\ (h - h_f)^m$, where A, h_f and m are fitting parameters. Meyer hardness (H) and effective modulus of contact (E_{eff}) can be assessed based on their relationship with the contact area and the measured contact stiffness by

$$H = \frac{P_{max}}{A_c}, \tag{5}$$

$$E_{eff} = \frac{S}{\sqrt{A_c}}, \tag{6}$$

where A_c is the projected contact area of the indenter with the sample surface. For indentation against a homogeneous, isotropic, elastic half-space E_{eff} is related to material properties by

$$\frac{1}{E_{eff}} = \frac{1}{\beta}\left(\frac{1-\nu_s{}^2}{E_s} + \frac{1-\nu_d{}^2}{E_d}\right), \tag{7}$$

where E_d and ν_d are the Young's modulus (1137 GPa) and Poisson's ratio (0.07) of the diamond probe, and E_s and ν_s are the same quantities for the specimen. β is a constant that depends on the geometry of the indenter. Once the Poisson's ratio of the specimen (ν_s) is known, the elastic modulus of specimen (E_s) can be determined. However, it should be noted that for indentation against a layered elastic half-space (such as a thin film on a substrate), the first term in parentheses in Eq. (7) must be replaced by $1/E_r$, where E_r depends upon the size of the indent in relation to the layer.[24] As the indent size increases, the substrate of the thin film will have an increased effect on E_r. The value of the specimen's elastic modulus (E_s) calculated using Eq. (7) is usually overestimated and cannot be used directly. Several works have been reported for nanoindentation studies of the mechanical properties of porous low-k to ultralow-k dielectric films deposited on silicon wafers.[25,26] However, some of the measured results were unconvincing by inappropriately eliminating the effects of the hard substrate. Also, for the porous structure of SiCOH, film densification underneath the probe could be significant during the indentation process, which brings new challenges to nanoindentation analysis.

To obtain more reliable testing, some modifications were used in this work. First, the contact area (A_c) at each indentation depth (h) was optimized. After correcting the fused silica load (P)—depth (h) traces for machine compliance, the Oliver-Pharr method[27] was used to assess contact area based on initial unloading contact stiffness (S) and contact depth ($h_c = h - 0.75{*}P/S$) for each indent. Then, the area function (A_c) was determined by a calibration equation as follows:

$$A_c(h_c) = 24.5h_c{}^2 + C_1h_c + C_2h_c{}^{1/2} + C_3h_c{}^{1/4} + C_4h_c{}^{1/8} + C_5h_c{}^{1/16}, \tag{8}$$

where C_1-C_5 are calibration constants of the indenter tip determined by the indentations on fused silica. The substrate effects on the film elastic modulus (E) are accounted for by comparing the experimental E_{eff} as a function of indent size to Stone's theoretical simulations.[21] For the simulations, the Poisson's ratio of SiCOH was assumed to be 0.25,[28] and the elastic modulus and Poisson's ratio of the silicon substrate were taken to be

161 GPa and 0.227, respectively. The only fitting parameter here is the nanoindentation correction factor—β, which is dependent on the indenter geometry, tip bluntness, and Poisson's ratio of the material being indented, which was determined to equal 1.23 following previous work.[29–31]

Figure 5 shows the comparison of experimental E_{eff} (solid symbols) of the differently annealed as-deposited SiCOH films under a humidity level of 10% with calculated E_{eff} (open symbols) using Stone's model. The abscissa is the square root of the contact area ($\sqrt{A_c}$) normalized by film thickness (h_f), which enables the simulations to be compared with films of arbitrary thickness. A method used by other researchers to assess SiCOH film E_s was to identity a "plateau" region at small loads in which it was assumed the substrate had negligible effect.[25,32] However, our experimental E_{eff} does not display a plateau and the simulated E_{eff} confirms that a plateau would not be expected for these experiments. In the absence of the plateau region, a model must be relied upon to accurately assess the value of E_s for SiCOH.[25,26,33] Here, we rely on Stone's model and in Figure 5 the agreement between experimental and the simulated E_{eff} is good when $\sqrt{A_c}/h_f$ is less than 1. Above $\sqrt{A_c}/h_f$ the experimental E_{eff} are higher than the simulated E_{eff}. The data suggest that in addition to substrate effects, the porous SiCOH is also densifying under the nanoindenter probe and above the hard Si substrate, which causes an increase in stiffness as suggested by previous researchers.[33]

When $\sqrt{A_c}/h_f$ is less than 1.0, the good agreement between experimental and simulated results indicates densification does not have a significant effect. Consequently, only data obtained in this region is used in the analysis, to guarantee the measured values are characteristics of the porous SiCOH films not the densified layer. Taking the water-saturated as-deposited SiCOH at a humidity of 10% as an example, the experimental measured elastic modulus, as shown in Figure 4, located between two simulated plots of $E_s = 5.0$ GPa and $E_s = 6.0$ GPa in the region of $\sqrt{A_c}/h_f < 1.0$, corresponding a true modulus value of 5.3 $\pm$ 0.2 GPa. The true effective elastic moduli of other treated SiCOH samples can be obtained in a similar way.

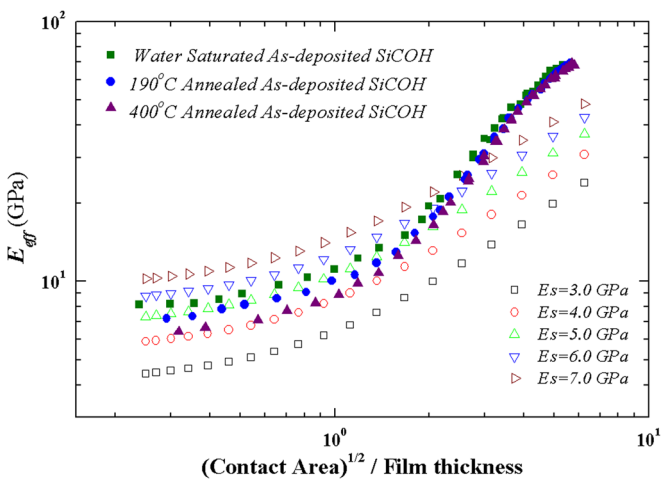

FIG. 5. Comparison of experimental E_{eff} (solid symbols) of the water-saturated as-deposited SiCOH film under a humidity level of 73% with simulated E_{eff} (open symbols) from Stone's model.

Figure 6 shows the measured hardness of SiCOH films as a function of the square root of the indentation contact area normalized by film thickness. It was found that these hardness curves, both as-deposited and UV-cured SiCOH, look qualitatively similar, independent of the annealing condition and humidity. At the onset of the indentation test, the curves level off and the measured hardness stays at a plateau value for shallow indentation depths. Then, the measured hardness begins to increase significantly with increased load. Finally, when the indenter probe approaches the film and substrate interface, a discontinuity (a sudden drop) in hardness appears in the curve. These discontinuities should be attributed to the pop-in events[32] (when the indentation depth becomes large). As shown in Figure 3(b), pop-in events occur (indicated by arrows) for indentation depths of about 310 nm for water-saturated UV-cured SiCOH under humidity of 73%. Load-depth traces with different maximum loads show that all pop-ins begin at the same indentation depth. The pop-in events appear for both as-deposited and UV-cured samples, and likely result from the film cracking and adhesion loss (delamination) between the film and substrate.[23] Since hardness assesses the resistance of the material to plastic deformation underneath the indenter, when a crack forms, the probe can more easily penetrate into the film/substrate system. This degenerated resistance induces a substantial increase in the contact area and a significant reduction in measured hardness, so a discontinuity appears in the hardness curve.

To coincide with the elastic modulus, we also chose $\sqrt{A_c}/h_f < 1.0$ as the hardness effective range, which is situated in the plateau region. The effective hardness of the film can be determined by the plateau value. For simplicity, we assume the plateau region is the "top layer" of the film and the discontinuity region as "bottom layer" of the film.

It should be noted that in the hardness effective range ($\sqrt{A_c}/h_f < 1.0$), the hardness results for UV-cured SiCOH are

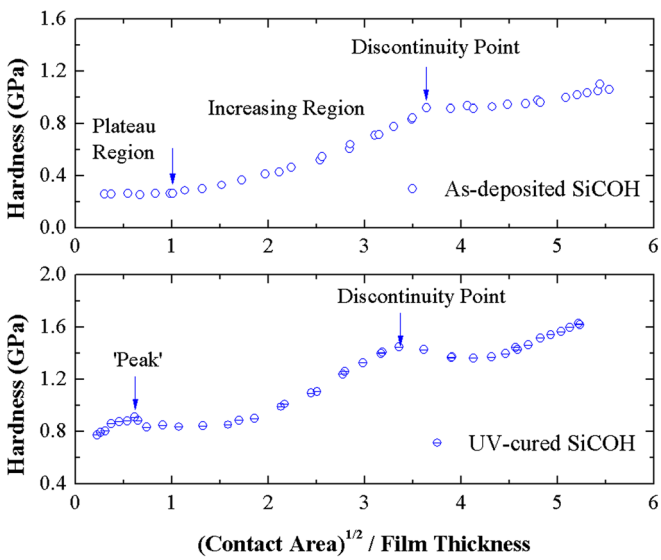

FIG. 6. Measured hardness of SiCOH films as a function of indentation contact radius normalized by film thickness. The data are based on the measurement on 400 °C annealed as-deposited and UV-cured SiCOH under humidity of 10%.

somewhat complex, compared with as-deposited SiCOH, for which the hardness increases and then decreases with the indentation depth, forming a peak located at about $\sqrt{A_c}/h_f = 0.6$. Similar phenomena were observed for all UV-cured SiCOH samples. It is not clear at present whether this scenario is caused by UV-curing induced non-uniform structural rearrangements on the film upper interfaces or whether it is related to differences in the hardness/modulus ratio that controls the plasticity region beneath the probe. So a relative percentage change of the film hardness for UV-cured SiCOH could be used instead of the exact hardness value.

B. Mechanical properties

1. Elastic modulus

Table III summaries the indenter-measured elastic moduli of dehydrated SiCOH films under humidity of 10%, using the calibration methods discussed in the above section. As discussed earlier, the roles of α-bonded and β-bonded water can be identified by comparing the properties of the annealed SiCOH samples at low humidity.

As listed in Table III, the tested elastic modulus varies with the absorbed water components for as-deposited SiCOH films. Water-saturated films (with both α- and β-bonded water in the bulk) have the highest E_s of 5.5 ± 0.2 GPa, α-bonded water removed films have a lower E_s of 5.1 ± 0.2 GPa, and both α- and β-bonded water removed films have the lowest E_s of 4.2 ± 0.2 GPa. These results indicate that reduced water in the SiCOH decreases the film's elastic modulus, which is consistent with the results of Broussous *et al.*[7] Further analysis shows that, compared with the water-saturated samples, the elastic modulus of samples with only β-bonded water does not decrease substantially (7.3%), while for the both α- and β-bonded water-removed sample, the E_s value has a larger drop (23.6%). The decrease in the modulus for initially both α- and β-bonded water removed SiCOH is more than three times of that for only α-bonded water removed SiCOH. This may indicate that the β-bonded water has a more significant effect on the elastic modulus than α-bonded water for as-deposited SiCOH.

After conditioning at higher RH, the water-saturated SiCOH film shows no difference in elastic modulus since the hydrophilic groups are all both α- or β-bonded and no more water can be absorbed. However, for the dehydrated SiCOH films, there is a significant change in the modulus with humidity. The elastic modulus variation induced by dehydration is offset by water from the increased humidity. After conditioning at an RH of 38%, the E_s decrease for 190 °C annealed SiCOH is around 3.6% compared with water-saturated SiCOH, while for 400 °C annealed SiCOH, this value is 10.9%. After conditioning at an RH of 73%, the moduli of the annealed samples are almost same as the water-saturated sample, indicating that the decrease in E_s associated with dehydration is reversible under these annealing conditions.

This can be explained as follows. Due to the annealing, there are lots of hydrophilic hydroxyl groups existing in the SiCOH as a consequence of the dehydration of α- and β-bonded water. At low humidity, little water reabsorption occurs. When the humidity is slightly increased, the water density gradient between the atmosphere and the films is small, so that the possibility of water molecules being reabsorbed by hydroxyl bonds is also small. Thus, dehydrated films show just a slight increase in their modulus when the humidity increases from 10% to 38%. As the humidity increases to 73%, more water from the atmosphere can be absorbed and incorporated into the film. The reabsorbed water molecules tend to exist in the β-bonded form, because at the beginning, the number of hydrophilic hydroxyl bonds should be larger than the number of water molecules. Under these conditions, the water tends to be bonded tightly to neighboring hydroxyl groups with two hydrogen bonds (β-bonded) until all of the hydroxyl groups are water-bonded and saturation is reached. This additional bonded water contributes to the increase of the elastic modulus. It is thus likely that when the humidity continues going higher, the elastic moduli of the dehydrated films will return to their initial levels. This result thus shows that increased water concentration increases the moduli of as-deposited SiCOH until saturation is reached.

For UV-cured SiCOH, the behavior of the elastic moduli of the annealed samples stands in contrast with as-deposited SiCOH. As shown in Table III, the measured elastic modulus of dehydrated UV-cured SiCOH conditioned at 10% RH is higher than that of the water-saturated samples. The measured elastic moduli of water-saturated SiCOH, initial α-bonded water removed and initial both α- and β-bonded water-removed UV-cured SiCOH conditioned at an RH of 10% were 6.0 ± 0.1 GPa, 6.2 ± 0.1 GPa, and 6.5 ± 0.1 GPa, respectively. Comparing with the water-saturated sample,

TABLE III. Measured elastic modulus for different annealed SiCOH at shallow indentation depth. The percentage increase or decrease in the elastic modulus compared with the reference water-saturated sample under a humidity of 10%.

		Elastic modulus (GPa)		
Dielectric films and treatments		10%	38%	73%
As-deposited	Water-saturated	5.5 ± 0.2 (–)	5.5 ± 0.2 (→)	5.5 ± 0.2 (→)
	190 °C annealed	5.1 ± 0.2 (7.3% ↓)	5.3 ± 0.2 (3.6% ↘)	5.5 ± 0.2 (→)
	400 °C annealed	4.2 ± 0.2 (23.6% ↓)	4.9 ± 0.2 (10.9% ↓)	5.3 ± 0.2 (3.6% ↘)
UV-cured	Water-saturated	6.0 ± 0.1 (–)	6.0 ± 0.1 (→)	6.0 ± 0.1 (→)
	190 °C annealed	6.2 ± 0.1 (3.3% ↗)	6.1 ± 0.1 (1.7% ↗)	6.0 ± 0.1 (→)
	400 °C annealed	6.5 ± 0.1 (8.3% ↑)	6.3 ± 0.1 (5.0% ↗)	6.1 ± 0.1 (1.7% ↗)

[a]The percentage increase/decrease was calculated based on the results of water-saturated sample after 10% RH conditioning.

the dehydration of only α-bonded water increases E_s by 3.3%, and when both α- and β-bonded water were removed, the increase was 8.3%, as listed in Table III. These variations are much smaller than as-deposited SiCOH, indicating water uptake has a smaller effect on UV-cured SiCOH.

These different responses to water absorption/desorption are believed to be because of UV curing. UV curing on SiCOH at elevated temperatures provides radiation excitation and thermal energy to stabilize the film structure by the removal of entrapped volatile hydrocarbons (-CH_3) and through local bond rearrangements, e.g., the transition of large angle Si-O-Si bonds to more stable small angle ones.[10] Under these conditions, the weak hydrophilic terminal bonds of Si-OH can be severed and replaced with hydrophobic cross-linked Si-O-Si bonds.[10,28] This lower density of hydrophilic bonds (-Si-OH) will lower the dissolution of water in the film and reduce the possibility of water absorption from humid ambient. This is also confirmed by examining the FTIR spectrum of UV-cured SiCOH in Figure 2(b), where the -OH related peak is much lower than that for as-deposited SiCOH. Thus, for UV-cured SiCOH, the film's elastic modulus shows a weaker dependence on water uptake in an aqueous environment.

Furthermore, these water-related moduli variations were shown to be reversible, since when the humidity was increased, the modulus of dehydrated UV-cured SiCOH was shown to approach that of water-saturated samples, and therefore the modular differences between various annealed samples can be negligible when the films were conditioned at 73% RH.

2. Film hardness

The hardness of the different annealed SiCOH films, both as-deposited and UV-cured, was also measured and analyzed, respectively, under varying humidity conditions. Table IV summaries the measured hardness (H) at shallow indentation depths under different humidity, for both as-deposited and UV-cured SiCOH.

For as-deposited SiCOH, the H of water-saturated, when only α-bonded water was removed and when both α- and β-bonded water was removed were measured to be 0.35 ± 0.01 GPa, 0.32 ± 0.01 GPa, and 0.27 ± 0.01 GPa, respectively, after 10% RH conditioning. Compared with the water-saturated samples, dehydration of only α-bonded water and dehydration of both α- and β-bonded water induces hardness degradations of 8.6% and 22.8% separately, demonstrating that dehydration of SiCOH decreases the hardness. In addition, the β-bonded water has a more significant effect than α-bonded water. These variation trends are in good agreement with that for the elastic modulus for as-deposited SiCOH. When the film were conditioned at 38% and then 73% RH, the hardness of the water-saturated SiCOH film almost remains stable; while for the dehydrated films, the hardness increases and tends to approach the value of the water-saturated samples, as shown in Table IV. It can be concluded that the decreases in film hardness caused by dehydration can be reversed by conditioning at higher RH.

For UV-cured SiCOH, because of the volatility of the UV-cured hardness, the relative percentage variation (%) for H is used instead of the averaged values. These are shown in Table IV. Dehydration of the UV-cured samples comes with enhanced hardness. For example, after 10% RH conditioning, the 400 °C annealed sample, from which both α- and β-bonded water was removed, has a 16.7% increase in hardness compared with the water-saturated sample. For the 190 °C annealed sample, an increasing of 13.6% was found. On the other hand, when the humidity of the water-saturated sample was increased, their hardness remains almost the same. For dehydrated samples annealed at either 190 °C or 400 °C, the enhanced hardness can be offset by water reabsorption in increased humidity, illuminating the water-dependent hardness variation is also reversible. Thus, the hardness increases when the water was removed by annealing. This coincides with the trend for the elastic modulus variation with humidity discussed in Sec. III B 1.

However, a more significant water-related hardness variation was observed when the samples were subjected to a high load indentation test, where cracking appears in the film. Figure 7 shows the measured hardness of various pretreated as-deposited SiCOH films, as a function of square root of the indentation contact area normalized to the film thickness. The arrows indicate the first occurrence of a cracked indent. The most significant difference appears in the discontinuity region where cracked indents occur on the sample, corresponding to the film "bottom layer" defined previously. It shows that: (1) the dehydration of water from SiCOH films results in a higher measured "bottom layer" hardness. The high-load indentation test after conditioning at 10% RH illustrates that α- and β-bonded water-removed samples show the highest measured "bottom layer" hardness,

TABLE IV. Measured hardness for different annealed SiCOH at shallow indentation depth. The percentage increase or decrease in the elastic modulus is compared with the reference: water-saturated sample under humidity of 10%.

Dielectric films and treatments		Hardness (GPa)		
		10%	38%	73%
As-deposited	Water-saturated	0.35 ± 0.03 (–)	0.35 ± 0.02 (→)	0.35 ± 0.02 (→)
	190 °C annealed	0.32 ± 0.02 (8.6% ↓)	0.34 ± 0.02 (2.9% ↘)	0.35 ± 0.02 (→)
	400 °C annealed	0.27 ± 0.01 (22.8% ↓)	0.31 ± 0.02 (11.4% ↓)	0.33 ± 0.02 (5.7% ↓)
UV-cured	Water-saturated	—	→	→
	190 °C annealed	13.6% ↑	6.1% ↑	3.0% ↗
	400 °C annealed	16.7% ↑	7.6% ↑	4.5% ↗

[a]The percentage increase/decrease was calculated based on the results of water-saturated sample after 10% RH conditioning.

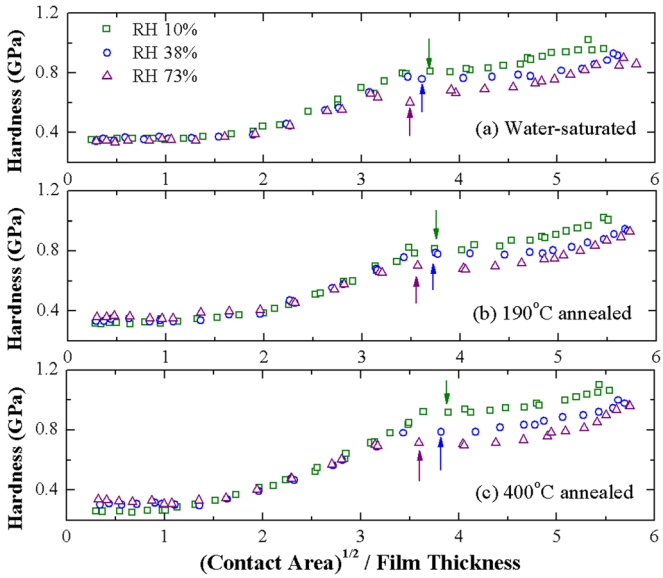

FIG. 7. High loading indentation test measured hardness of different pretreated as-deposited SiCOH films, as a function of square root of the indentation contact area normalized to the film thickness. Labeled arrows indicate the first occurrence of cracked indent.

followed by the α-bonded water-removed samples and then by the water-saturated samples. (2) For both dehydrated and water-saturated samples, the measured "bottom layer" hardness substantially decreases with increased humidity. The same phenomena are observed with a high load test on UV-cured SiCOH films, as shown in Figure 8.

The distinctions between measured "bottom layer" hardness for different samples are attributed to the water induced characteristics variations of the film-substrate interface. In-diffused water at the SiCOH/Si interface has a significant detrimental effect on adhesion between SiCOH and substrate.[34] When SiCOH/Si stacks are exposed to an aqueous environment, the adhesion energy of the film-substrate interface degrades drastically as a result of the in-diffusion of water. The degradation of adhesion energy results in a weaker film/substrate interaction and a subsequently weaker resistance of the dielectric results in various forms of fracture caused by stress.[35] As a consequence, the measured "bottom layer" hardness can be intimately linked to the water concentration at the film/substrate interface. Under a high-load indentation test, samples with lower water concentration at the film-substrate interface have a higher crack resistance and hardness degradation is less significant. The higher measured "bottom layer" hardness of the 400 °C-annealed samples after 10% RH conditioning sustains this scenario.

The crack profiles shown in SEM images of various indents also support this inference. Figure 9 shows the measured fracture length (c) of each crack under a high-load test for as-deposited and UV-cured samples, respectively. The arrows indicate the location of the first observed crack on the film. Thus, annealing of the sample improves the threshold load for film cracking. The 400 °C-annealed sample exhibits

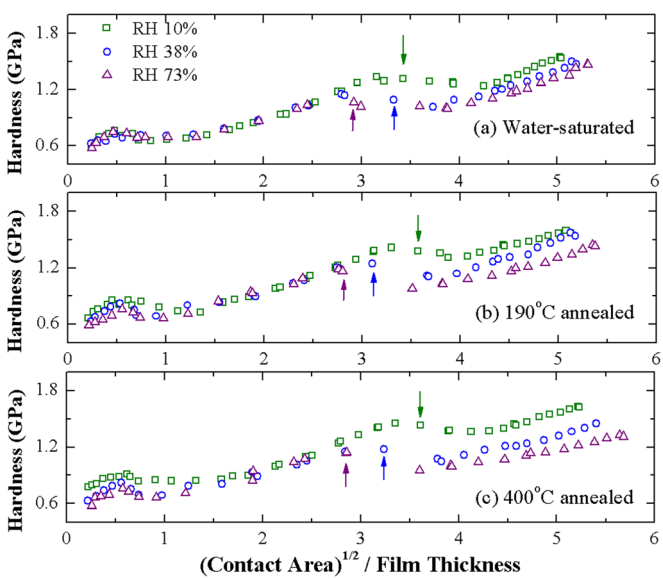

FIG. 8. High loading indentation test measured hardness of different pretreated UV-cured SiCOH films, as a function of indentation square root of the indentation contact area normalized to the film thickness. Labeled arrows indicate the first occurrence of cracked indent.

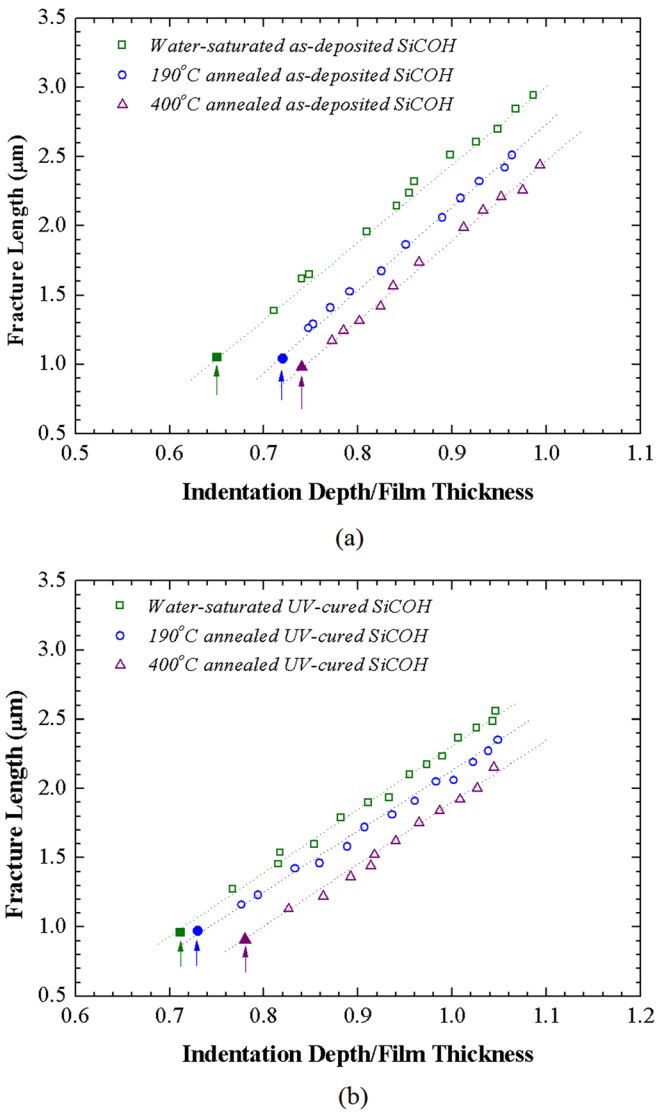

FIG. 9. (a) Fracture length of each crack under high loading test for as-deposited sample after 10% RH conditioning. (b) Fracture length of each crack under high loading test for UV-cured sample after 10% RH conditioning. Arrows indicate the observed first crack.

TABLE V. Crack threshold indentation depth normalized by film thickness for indentation on different samples.

Dielectric films and treatments		Crack threshold[a]		
		10%	38%	73%
As-deposited	Water-saturated	0.66 (–)	0.65 (1.5% ↘)	0.62 (6.1% ↓)
	190 °C annealed	0.72 (9.1% ↑)	0.70 (6.1% ↑)	0.66 (→)
	400 °C annealed	0.74 (12.1% ↑)	0.71 (7.6% ↑)	0.67 (1.5% ↗)
UV-cured	Water-saturated	0.71 (–)	0.69 (2.8% ↘)	0.67 (5.6% ↓)
	190 °C annealed	0.73 (2.8% ↗)	0.71 (→)	0.70 (1.4% ↘)
	400 °C annealed	0.78 (9.9% ↑)	0.76 (7.0% ↑)	0.73 (2.8% ↗)

[a]Crack threshold is defined as the ratio of indentation depth to film thickness at which crack is observed for the first time to the film thickness.
[b]The percentage increase/decrease was calculated based on the results of water-saturated sample after 10% RH conditioning.

the highest crack threshold indentation depth, followed by the 190 °C annealed and the water-saturated samples. Examining the as-deposited SiCOH after 10% RH conditioning, for example, when the indentation depth reaches 70% of the film depth, cracking is observed on the water-saturated sample, while the 190 °C and 400 °C annealed samples are still crack free. This shows that annealing can effectively reduce the water concentration in the film/substrate interface and enhance the adhesion between them, resulting in increased crack resistance. This is consistent with the results that the annealed samples have a higher measured "bottom layer" hardness and the water-saturated samples show degraded properties under a high-load test.

Table V summarizes the crack-threshold indentation depth normalized by film thickness for measurements under different humidities. As can be seen, increased humidity offsets the annealing strengthening effect, since in aqueous environments lateral water diffusion along the SiCOH/Si interface is significant[6] and in-diffused water inherently degrades the adhesion energy. That is why the "bottom layer" hardness, measured with a high-load test, substantially decreases when the humidity increases, as shown in Figures 8 and 9. This decrease is also observed in the water-saturated samples, for which increased humidity shows no effect on the "top layer" hardness. This is because when the film is cracked, the SiCOH/Si surface is almost directly exposed to the aqueous ambient. Instead of diffusion staring from the sample edge/upper surface and then through the whole film layer, water from the aqueous environment can directly reach the film/substrate interface and stay there. The "in-diffused" water concentration at the film/substrate interface will significantly increase. As a consequence, the measured "bottom layer" hardness shows a substantial decrease with increased humidity, for both the water-saturated and annealed samples.

These observations suggest that cracking of the film can provide a new diffusion path for ambient water. The "bottom layer" hardness of SiCOH/Si stacks is highly related to the in-diffused water concentration at the film/substrate interface. Tests on both as-deposited and UV-cured SiCOH show the same trends.

One somewhat surprising aspect is that the water induced film/substrate adhesion degradation has far less effect on the elastic modulus than on the hardness, as depicted in Figures 10 and 11. This should be because the

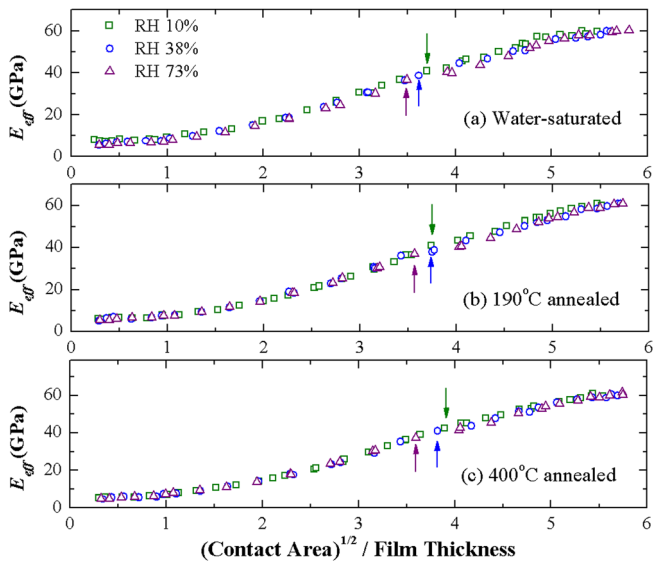

FIG. 10. High loading indentation test measured elastic modulus of different pretreated as-deposited SiCOH films, as a function of square root of the indentation contact area normalized to the film thickness. Labeled arrows indicate the first occurrence of cracked indent.

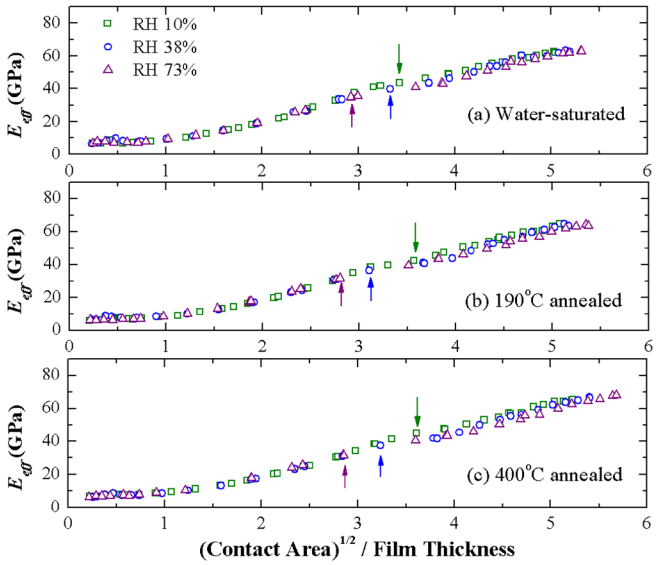

FIG. 11. High loading indentation test measured elastic modulus of different pretreated UV-cured SiCOH films, as a function of square root of the indentation contact area normalized to the film thickness. Labeled arrows indicate the first occurrence of cracked indent.

elastic modulus depends directly on the ratio of stiffness to the square root of the contact area. When water diffuses into the SiCOH/Si surface, the hardness decreases, meaning that the contact area between the indenter and the specimen increases. With a larger contact area, we also measure a larger stiffness, and as a result, we do not see much change in the elastic modulus after in-diffusion of water. Thus, no substantial decrease of the measured elastic modulus with increased humidity was observed when the film was cracked.

IV. CONCLUSION

In summary, the influence of water uptake on the mechanical properties of low-k organosilicate glass was investigated with nanoindentation. For as-deposited PECVD SiCOH, the effects of absorbed water on elastic modulus and on hardness qualitatively hold the same evolution mechanism. UV curing is shown to effectively lower water-induced mechanical property variations, by depopulating the hydrophilic chemical groups in SiCOH. A high-load indentation test shows that in-diffusion of water along the film/substrate interface can degrade the hardness of a SiCOH/Si film stack significantly. The elastic modulus, however, shows a smaller dependence on in diffusion of water.

ACKNOWLEDGMENTS

This work was supported by the Semiconductor Research Corporation under Contract No. 2012-KJ-2359, by the National Science Foundation under Grant No. CBET-1066231, and by the Applied Materials University Research Partnership Program.

[1]K. Maex, M. R. Baklanov, D. Shamiryan, F. Iacopi, S. H. Brongersma, and Z. S. Yanovitskaya, J. Appl. Phys. **93**, 8793 (2003).
[2]M. R. Baklanov and K. Maex, Philos. Trans. R. Soc. London, Ser. A **364**, 201 (2006).
[3]A. Grill, J. Appl. Phys. **93**, 1785 (2003).
[4]D. Shamiryan, M. R. Baklanov, S. Vanhaelemeersch, and K. Maex, J. Vac. Sci. Technol. B **20**, 1923 (2002).
[5]J. Shoeb and M. J. Kushner, J. Vac. Sci. Technol. A **30**, 041304 (2012).
[6]H. Li, T. Y. Tsui, and J. J. Vlassak, J. Appl. Phys. **106**, 033503 (2009).
[7]Y. Li, I. Ciofi, L. Carbonell, N. Heylen, J. V. Aelst, M. R. Baklanov, G. Groeseneken, K. Maex, and Z. Tokei, J. Appl. Phys. **104**, 034113 (2008).
[8]J. R. Lloyd, T. M. Shaw, and E. G. Liniger, in *Proceedings of IEEE International Integrated Reliability Workshop Final Report* (2005), p. 39.
[9]L. Broussous, G. Berthout, D. Rebiscoul, V. Rouessac, and A. Ayral, Microelectron. Eng. **87**, 466 (2010).
[10]F. Iacopi, Y. Travaly, B. Eyckens, C. Waldfried, T. Abell *et al.*, J. Appl. Phys. **99**, 053511 (2006).
[11]D. M. Gage, E. P. Guyer, J. F. Stebbins, Z. Cui, A. A. Bayati, A. Demos, K. P. MacWilliams, and R. H. Dauskardt, in *Interconnect Technology Conference* (2006), p. 149.
[12]L. L. Chapelon, J. Vitiello, J. P. Gonchond, D. Barbier, and J. Torres, Microelectron. Eng. **83**, 2136 (2006).
[13]J. Yao, A. Iqbal, H. Juneja, and F. Shadman, J. Electrochem. Soc. **154**, G199 (2007).
[14]H. Ren, G. A. Antonelli, Y. Nishi, and J. L. Shohet, J. Appl. Phys. **108**, 094110 (2010).
[15]J. Proost, E. Kondoh, G. Vereecke, M. Heyns, and K. Maex, J. Vac. Sci. Technol. B **16**, 2091 (1998).
[16]J. Proost, M. Baknalov, K. Maex, and L. Delaey, J. Vac. Sci. Technol. B **18**, 303 (2000).
[17]T. Sumomogi, K. Hieda, T. Endo, and K. Kuwahara, Appl. Phys. A **66**, S299 (1998).
[18]J. G. Park, S. H. Lee, B. Kim, and Y. W. Park, Appl. Phys. Lett. **81**, 4625 (2002).
[19]M. R. Baklanov, J. F. Marneffe, D. Shamiryan, A. M. Urbanowicz, H. Shi, T. V. Rakhimova, H. Huang, and P. S. Ho, J. Appl. Phys. **113**, 041101 (2013).
[20]C. Kubasch, H. Schumacher, H. Ruelke, U. Mayer, and J. W. Bartha, IEEE Trans. Electron Devices **58**, 2888 (2011).
[21]D. S. Stone, K. B. Yoder, and W. D. Sproul, J. Vac. Sci. Technol. A **9**, 2543 (1991).
[22]J. B. Vella, I. S. Adhihetty, K. Junker, and A. A. Volinsky, Int. J. Fract. **119/120**, 487 (2003).
[23]J. J. Kruzic, D. K. Kim, K. J. Koester, and R. O. Ritchie, J. Mech. Behav. Biomed. Mater. **2**, 384 (2009).
[24]D. S. Stone, J. Mater. Res. **13**, 3207 (1998).
[25]K. Vanstreels and A. M. Urbanowicz, J. Vac. Sci. Technol. B **28**, 173 (2010).
[26]C. Gaire, Y. Ou, H. Arao, M. Egami, A. Nakashima, R. C. Picu, G. C. Wang, and T. M. Lu, J. Porous Mater. **17**, 11 (2010).
[27]W. C. Oliver and G. M. Pharr, J. Mater. Res. **7**, 1564 (1992).
[28]A. Grill, Annu. Rev. Mater. Res. **39**, 49 (2009).
[29]J. E. Jakes, C. R. Frihart, J. F. Beecher, R. J. Moon, P. J. Resto, Z. H. Melgarejo, O. M. Suarez, A. A. Elmustafa, and D. S. Stone, J. Mater. Res. **24**, 1016 (2009).
[30]K. Tapily, J. E. Jakes, D. Gu, H. Baumgart, and A. A. Elmustafa, Int. J. Surf. Sci. Eng. **5**, 193 (2011).
[31]K. B. Yoder, D. S. Stone, R. A. Hoffman, and J. C. Lin, J. Mater. Res. **13**, 3214 (1998).
[32]L. Wang, M. Ganor, S. I. Rokhlin, and A. Grill, J. Mater. Res. **20**, 2080 (2005).
[33]H. Li and J. J. Vlassak, J. Mater. Res. **24**, 1114 (2009).
[34]Y. Lin, T. Y. Tsui, and J. J. Vlassak, J. Electrochem. Soc. **157**, G53 (2010).
[35]T. Y. Tsui, A. J. McKerrow, and J. J. Vlassak, J. Mech. Phys. Solids **54**, 887 (2006).